Journal of Materials Chemistry

Dynamic Article Links

Cite this: *J. Mater. Chem.*, 2011, **21**, 16544

www.rsc.org/materials

PAPER

In situ production of high filler content graphene-based polymer nanocomposites by reactive processing

Valeria Alzari,[a] Daniele Nuvoli,[a] Roberta Sanna,[a] Sergio Scognamillo,[a] Massimo Piccinini,[b] Josè Maria Kenny,[c] Giulio Malucelli*[d] and Alberto Mariani*[a]

Received 12th May 2011, Accepted 22nd August 2011
DOI: 10.1039/c1jm12104a

This work deals with the preparation of graphene dispersed in a monomer (tetraethylene glycol diacrylate) and the subsequent polymerization of the latter to the corresponding polymer nanocomposite, which is the first obtained so far by direct polymerization of the graphene-dispersing medium. The method used for its obtainment allows reaching the highest concentration of graphene reported until now in any medium (9.45 mg mL^{-1}); besides, a certain amount of graphene nanoribbons is also well visible. Furthermore, this goal is achieved by directly sonicating graphite without any chemical manipulation, which generally results in a final material still containing a significant number of defects. Because of its obtainment in the monomer itself, no filtration of graphene is needed, thus avoiding the reaggregation process to graphite, which partially compromises any previous exfoliation process. The obtained graphene-based polymer nanocomposites, fully characterized by Raman and transmission electron microscopy, differential scanning calorimetry, thermogravimetry, and dynamic–mechanical thermal analysis, exhibit a very homogeneous distribution of the graphene sheets within the polymer matrix. In addition, the interactions between the polymer and nanofiller are very strong, as evidenced by a significant increase in the T_g values even in the presence of a very low graphene content, together with a strong increase in the mechanical features (flexural and storage moduli). Finally, the thermo-oxidative stability of the polymer matrix is not affected by the presence of graphene nanosheets.

Introduction

Graphene, a monolayer of sp^2-hybridized carbon atoms arranged in a two-dimensional lattice, is currently the material that attracts most of the interest of both breakthrough research and media. Actually, graphene had already been theoretically studied from 1947 by Wallace[1] as an example for calculations for students of solid state physics. However, only theoretical studies were performed until 2004 when Geim and Novoselov (who were awarded the 2010 Nobel Prize in Physics "*for groundbreaking experiments regarding the two-dimensional material graphene*") presented their results on graphene structures.[2] Since 2005, the studies in this research area have literally exploded, producing an increasingly growing number of papers concerning graphene and its outstanding features, namely a high Young's modulus (~1100 GPa),[3] fracture strength (125 GPa),[3] thermal conductivity (5×10^3 W m^{-1} K^{-1}),[4] mobility of charge carriers (2×10^5 cm^2 V^{-1} s^{-1})[5] and the specific surface area (2630 m^2 g^{-1}).[6]

Nevertheless, the development of graphene-based technologies strictly depends on an efficient approach for obtaining graphene sheets in large quantities. In particular, the methods used for graphene preparation involve mechanical cleavage of graphite,[7] epitaxial growth using chemical vapor deposition,[8] thermal pyrolisis of polycyclic aromatic hydrocarbons,[9] and the explosive oxidation of graphite followed by the reduction of graphene oxide.[10] As a matter of fact, most of the above methods are characterized by low productivity, which makes them unsuitable for a large-scale use.[10] In this respect, the most effective and promising route for their bulk production is the exfoliation of graphite in a liquid medium to form single or few-layered graphene sheets. On the basis of a pioneering work by Hernandez *et al.*,[11] who succeeded in obtaining graphene sheets by direct graphite exfoliation in *N*-methylpyrrolidone (NMP), other groups have developed this promising method.[12–17] In particular, starting from the initial concentration of 0.01 mg mL^{-1} reported by Hernandez *et al.*,[15] our research group was able to achieve the highest graphene concentration reported so far (5.33 mg mL^{-1}) by dispersing graphene in a suitable ionic liquid.[18]

The use of such a nanofiller for obtaining polymer nanocomposites represents one of the most promising applications.

[a]*Dipartimento di Chimica, Università di Sassari, and local INSTM unit, Via Vienna 2, 07100 Sassari, Italy. E-mail: mariani@uniss.it*
[b]*Porto Conte Ricerche S.r.l., SP 55 km 8.400 Loc. Tramariglio, 07041 Alghero (SS), Italy*
[c]*ICTP-CSIC, Juan de la Cierva 3, 28006 Madrid, Spain*
[d]*Dipartimento di Scienza dei Materiali ed Ingegneria Chimica, Politecnico di Torino, sede di Alessandria, and local INSTM unit, Via T. Michel 5, 15121, Alessandria, Italy. E-mail: giulio.malucelli@polito.it*

This journal is © The Royal Society of Chemistry 2011

The earliest reports on polymer composites with exfoliated graphite fillers emerged from studies on graphite intercalation compounds (GICs).[19–21] In 1991, Bunnell patented the use of graphite nanoplatelets (GNPs) as fillers in polymer nanocomposites.[22] In 2000, a detailed study on an exfoliated graphite-based nanocomposite synthesized starting from ε-caprolactam was reported.[23] Also graphite oxide (GO) can be intercalated by different monomers[24] or polymers.[25] In recent years, a number of polymer nanocomposites were prepared by dispersing GNPs and GO-derived fillers in various polymeric matrices.[26]

However, melt and solvent processing routes reported do not provide reliable processes for graphene dispersion and distribution in their polymer matrix nanocomposites and, furthermore, they require a complex and difficult manipulation of graphene. In order to simplify and improve the feasibility of the use of graphene in polymer nanocomposites, its "*in situ*" dispersion obtained starting from graphite flakes in reactive media will be developed. Indeed, so far these materials have been obtained only by using graphene dispersed in inert solvents to be removed after the polymerization reaction.[27] In this respect, the highest graphene concentrations in non-reactive media are those reported by us in ref. 18 and 28. Namely, in NMP a graphene concentration equal to 2.21 mg mL^{-1} was achieved,[28] while in a suitable ionic liquid the aforementioned value of 5.33 mg mL^{-1} was found.[18] It should be highlighted that the previously highest values published by other groups were 1.2 mg mL^{-1} (in NMP),[14] and 2.0 mg mL^{-1} (in a very aggressive medium such as chlorosulfonic acid).[13]

On the basis of the method described in our previous works,[18,28] we decided to investigate the possibility of obtaining a high graphene concentration in polymerizing media.

In particular, in this work we report the first example of a polymer nanocomposite containing graphene dispersed directly into an acrylic monomer (namely, tetraethylene glycol diacrylate, TEGDA), thus avoiding any solvent removal and at the same time limiting graphene reaggregation. This liquid was selected because it was found to be the most effective in a series of several monomers having various functional groups. The obtained graphene-based nanocomposites were investigated as far as their morphology, thermal and mechanical properties are concerned. Significant improvements in such features were found when the graphene concentration in the liquid acrylic monomer was limited up to 4.67 mg mL^{-1}. Although it was possible to further increase the nanofiller content (reaching 9.45 mg mL^{-1}), the thermal and mechanical properties of the obtained polymer dramatically dropped, approaching the features of the neat polymer.

Results and discussion

Dispersion characterization

The first significant goal of the present work was to obtain high concentrations of graphene directly from graphite without any of the chemical manipulations reported in the literature.[7–10] Namely, no oxidation to graphene oxide followed by its reduction was carried out, this latter being a method that allows obtaining quite high nanofiller concentrations; however, since such a reduction is generally incomplete, some defects, which may partially compromise its peculiar features, remain on the graphene surface.[10]

Fig. 1 Tyndall effect measured on TEGDA/graphene dispersion (diluted 1 : 20).

A first indication of the nanometric dimensions of the dispersed graphene particles can be provided by the occurrence of the Tyndall effect. As shown in Fig. 1, light scattering confirms the colloidal nature of our TEGDA/graphene dispersion.

The concentration of graphene, determined by gravimetry after filtration, was as high as 9.45 mg mL^{-1}, which represents the highest value reported so far in any solvent and obtained by any method. It is noteworthy that our approach is not only very effective but also as simple as possible and by-passes the recovering of graphene from a non-reactive solvent, which partially compromises any previous successful step, since a partial reaggregation of the nanofiller to graphite flakes occurs.

Furthermore, it should be highlighted that, for the first time, graphene has been obtained in high concentration directly in the monomer to be polymerized for nanocomposite preparation. This result represents a big step forward that may pave the way toward the easy and convenient obtainment of these nanomaterials in a large scale.

In Fig. 2, the UV-VIS calibration curve for graphene/TEGDA dispersions is plotted: the system shows Lambert–Beer behavior, with an absorption coefficient of 436 mL mg^{-1} m^{-1}.

Raman spectroscopy is essential for the characterization of graphene, because not only it can discriminate between graphite

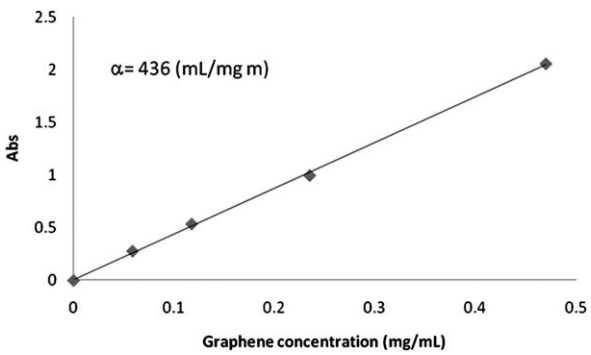

Fig. 2 Calibration curve for graphene/TEGDA dispersion.

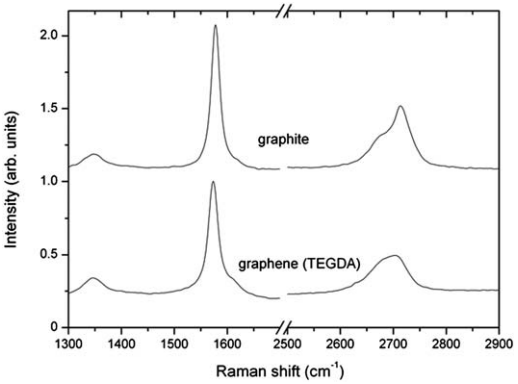

Fig. 3 Raman spectra of graphite (top line) and of the graphene obtained from TEGDA dispersion (bottom line).

and graphene, but also allows determining the number of layers.[17,29,30] As shown in Fig. 3, the Raman spectrum of graphene obtained by filtration of its dispersion in TEGDA shows the typical graphene bands, namely G at 1574 cm^{-1}, 2D at 2703 cm^{-1} and the disorder-related D band at 1350 cm^{-1}. The shape and position of the 2D band suggest that the sample under examination is constituted of few-layer graphene.[29] As a comparison, the shape of the 2D band of pristine graphite is very different and consists of two components with a stronger peak at 2713 cm^{-1}.

The TEGDA/graphene dispersion (diluted 1 : 40) was analyzed by transmission electron microscopy to confirm graphene formation. Fig. 4a shows a few sheets of few-layer graphene, and Fig. 4b evidences the presence of some nanoribbons. It is worthy to note that this is the first reported example in which graphene nanoribbons are obtained directly by simple graphite sonication; in addition, for the first time, graphene nanoribbons are obtained directly in a monomer. Indeed, these nanomaterials were previously obtained by a chemical route,[31]

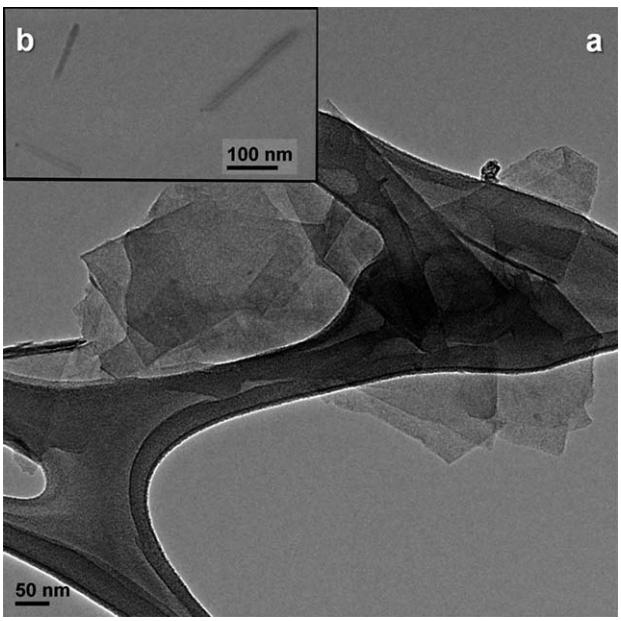

Fig. 4 TEM images of TEGDA/graphene dispersion (diluted 1 : 40): (a) a few sheets of few-layer graphene; (b) some nanoribbons.

Table 1 Graphene concentration in the obtained polymer nanocomposites

Sample name	Graphene concentration/mg mL^{-1}
23.1	0
23.4	0.12
23.3	0.43
23.2	4.67
34.1	9.45

by sonochemically cutting chemically derived graphene sheets,[32] by unzipping of nanotubes,[33] by using chlorosulfonic acid[13] and by a few other methods.[34]

Characterization of the graphene-based polymer nanocomposites

The compositions of all samples prepared in the present work are listed in Table 1.

Fig. 5 shows the Raman spectra of poly(TEGDA) (PTEGDA) (dashed line, sample 23.1) and PTEGDA containing graphene (solid line, sample 23.2); the spectra are normalized to the peak at 1730 cm^{-1}. The differences between these spectra are mainly due to graphene bands, in particular, the G band at 1580 cm^{-1} and the disorder-related D band at ~1350 cm^{-1}, which is superimposed on the PTEGDA spectrum. Furthermore, the other disorder-related D′ band peaked at 1630 cm^{-1} is now well visible. D and D′ bands are shifted and result better separated with respect to the spectrum of the graphene dispersion obtained from TEGDA monomer: such shift can be ascribed to the interaction between graphene and PTEGDA. Unfortunately, the 2D band at ~2700 cm^{-1} appears as a shoulder of the very strong PTEGDA Raman band peaked at ~3100 cm^{-1}; nevertheless, such a band is still typical of few-layer graphene because of its broadness and flatness, whereas the main peak of the graphite band would be much more intense and narrower.

Two typical SEM images of the fracture surfaces of neat PTEGDA (sample 23.1) and of a typical graphene-containing nanocomposite (sample 23.2) are displayed in Fig. 6.

In the latter, the presence of graphene sheets is clearly evident; in addition, while the surface of neat PTEGDA is quite smooth,

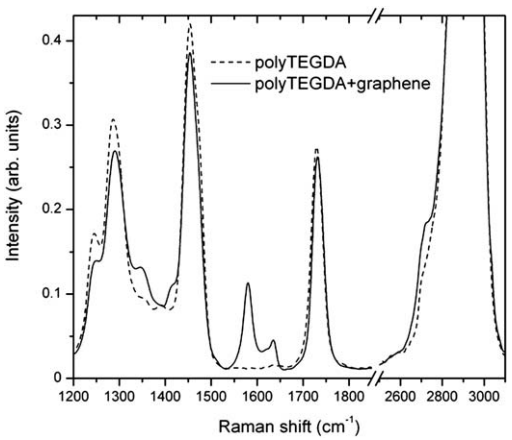

Fig. 5 Raman spectra of PTEGDA (dashed line, sample 23.1) and PTEGDA containing graphene (solid line, sample 23.2).

This journal is © The Royal Society of Chemistry 2011

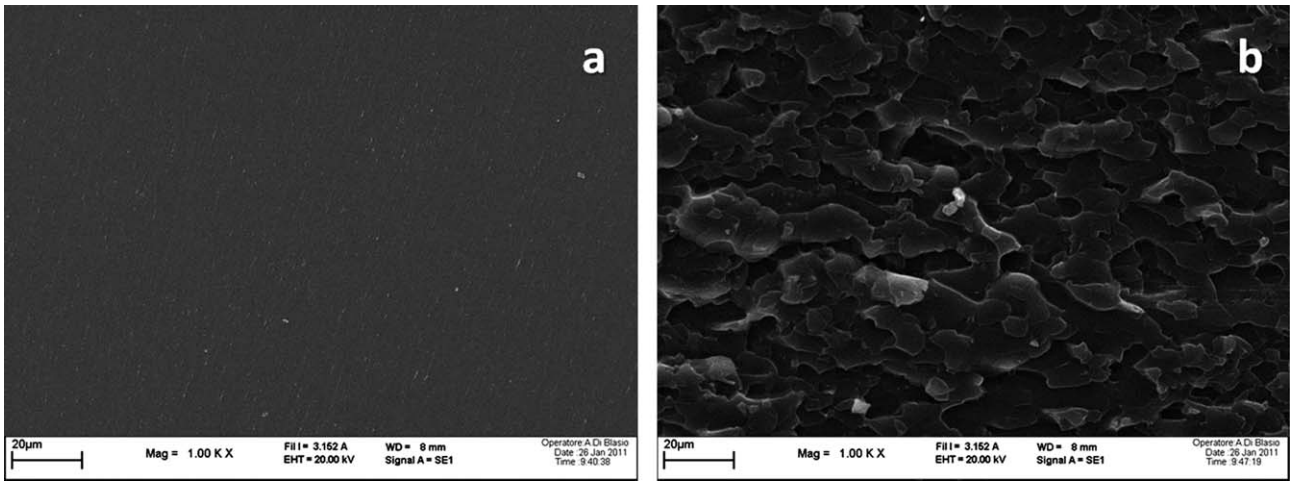

Fig. 6 a) Sample 23.1 (neat polymer) and (b) sample 23.2 (with 4.67 mg mL^{-1} of graphene).

that of the nanocomposite sample is very rough. It is also worthy to note that, regardless of their concentration in the polyacrylate network, a very homogeneous distribution of the graphene sheets within the polymer matrix is achieved for all the filled systems investigated, also including that characterized by the highest graphene content (not shown for brevity).

In Table 2, the glass transition temperatures (T_g) of neat PTEGDA and of its nanocomposites are listed.

The data clearly indicate that the T_g of the polymer is strongly affected by the presence of graphene nanosheets: indeed, T_g increases from 1 °C, for neat PTEGDA, up to 27 °C for sample 23.2, which contains 4.67 mg mL^{-1} of graphene. This finding is a clear indication of the effect of the nanofiller, which induces the formation of constraints that reduce polymer segments' mobility. Furthermore, the observed T_g trend seems to indicate that the interactions between graphene and the polymer matrix occur even at very low nanofiller content. Indeed, a significant 10 °C T_g increase is observed at the lowest graphene concentration (0.12 mg mL^{-1}, sample 23.4). In contrast, the presence of a very high amount of graphene (sample 34.1 of Table 2) causes a drastic reduction of the T_g value, which approaches that of pure PTEGDA. This finding can be attributed to the high concentration of graphene sheets within the polymer, which are responsible for a lubrication effect, thus increasing the mobility of the polymer segments and decreasing T_g. A similar behavior was evidenced by investigating the rheological properties of graphene-containing nanocomposite hydrogels of poly(*N*-isopropylacrylamide) prepared by frontal polymerization.[28]

Such a behavior was confirmed by DMTA analysis, which also pointed out a substantial increase in the storage modulus E', both in the glassy state and in the rubbery *plateau*, where the influence of the nanofiller on the mechanical behavior of the polymer matrix becomes larger (see Table 3 and Fig. 7). Once again, the only exception is observed for the sample with the highest graphene content (sample 34.1), which exhibits the T_g and E' values of the neat cured resin.

In order to further confirm the strong polymer/filler interactions, which graphene nanosheets are responsible for, flexural three point bending tests were performed at room temperature on all the prepared nanocomposites and the obtained results were compared with the unfilled counterpart. As collected in Table 3, a strong increase in flexural modulus is observed when graphene is added to the acrylic system: indeed, flexural modulus almost triples in the case of the nanocomposite with high nanofiller content (4.67 mg mL^{-1}), with respect to the unfilled material. In addition, a significant increase in the σ_{max} is achieved, as well. Also in this case, when the highest graphene content is added to the acrylic monomer (9.45 mg mL^{-1}), a strong decrease in the mechanical behavior (flexural modulus and σ_{max}, Table 3) is observed, in agreement with its T_g decrease (Table 2).

In Table 4, the results of TGA analyses performed in air are collected in terms of T5, T10 and T50, *i.e.* the temperatures at which the weight loss corresponds to 5, 10 or 50%, respectively. The collected data clearly indicate that the thermo-oxidative stability of the polymer is substantially not affected by the presence of graphene nanosheets, irrespective of the nanofiller content.

Table 2 Glass transition temperatures (T_g) and storage modulus (E') of the cured nanocomposites

Sample	Description	T_g DSC/°C	T_g DMTA/°C	E' (−50 °C)/MPa	E'(+100 °C)/MPa
23.1	Neat TEGDA	1.2	4.9	1639	11.4
23.4	TEGDA + graphene (0.12 mg mL^{-1})	10.7	13.8	1860	16.0
23.3	TEGDA + graphene (0.43 mg mL^{-1})	15.2	31.2	2370	26.3
23.2	TEGDA + graphene (4.67 mg mL^{-1})	26.9	48.7	2960	39.0
34.1	TEGDA + graphene (9.45 mg mL^{-1})	2.8	7.8	1715	13.3

Table 3 Flexural modulus and σ_{max} for the cured samples

Sample	Graphene content in PTEGDA/ mg mL^{-1}	Flexural modulus/ MPa	σ_{max}/MPa
23.1	0	58.7 ± 3.1	6.4 ± 2.6
23.4	0.12	51.2 ± 5.3	6.6 ± 3.1
23.3	0.43	80.6 ± 6.5	9.1 ± 2.7
23.2	4.67	170.5 ± 8.4	15.2 ± 1.9
34.1	9.45	56.9 ± 6.1	6.2 ± 2.7

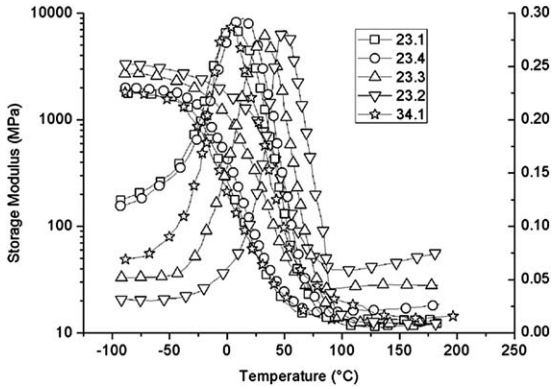

Fig. 7 DMTA traces of cured PTEGDA and its graphene polymer nanocomposites.

Experimental

Materials

Tetraethylene glycol diacrylate (TEGDA, M_w = 302.32, d = 1.11 g mL^{-1}) and graphite flakes were purchased from Sigma Aldrich and used as received without further purification.

Trihexyltetradecylphosphonium persulfate (TETDPPS) was used as the radical initiator and was synthesized according to the method described in the literature.[35]

Preparation of graphene nanocomposites

In order to prepare a graphene masterbatch dispersion, 5 wt% of graphite flakes were added to TEGDA, placed into a tubular plastic reactor (i.d. 15 mm) and ultrasonicated (Ultrasound bath EMMEGI, 0.55 kW, water temperature ~40 °C) for 24 h. Then the dispersion was centrifuged for 30 min at 4000 rpm; finally, the gray to black liquid phase containing graphene was recovered.

Table 4 TGA data of samples

Sample	Graphene content in PTEGDA/ mg mL^{-1}	T5/°C	T10/°C	T50/°C	Residue @800 °C (%)
23.1	0	345	375	419	1.7
23.4	0.12	356	380	416	0.5
23.3	0.43	354	378	414	0.8
23.2	4.67	351	376	418	1.1
34.1	9.45	348	372	416	1.2

The concentration of the dispersion, calculated by gravimetry after filtration through polyvinylidene fluoride filters (pore size 0.22 μm), was 9.45 mg mL^{-1}.

The above graphene masterbatch dispersion in TEGDA was analyzed by UV-VIS spectroscopy, using a Hitachi U-2010 spectrometer (1 mm cuvette), following the method reported in the literature.[15] Namely, a calibration line for graphene concentration was used, at a wavelength of 660 nm.[11,18,36] The calculated absorption coefficient was 436 mL mg^{-1} m^{-1}: this value was used for determining the actual graphene concentrations in any diluted dispersion derived from the masterbatch one.

As far as the preparation of the nanocomposite is concerned, the TEGDA/graphene masterbatch was further diluted with suitable amounts of TEGDA; then, 0.5 wt% of TETDPPS initiator was added and the polymerization was performed in Pasteur pipettes, used as tubular reactors, in an oven at 80 °C for 2 hours (see data in Table 1). Any run was repeated at least three times.

Characterization techniques

Raman spectroscopy was carried out with a Bruker Senterra Raman microscope, using an excitation wavelength of 532 nm at 5 mW. The spectra were acquired by averaging 5 acquisitions of 5 seconds with a 50× objective.

High resolution TEM images were obtained with JEOL equipment, model JEM-2010 operating with an acceleration voltage of 200 kV. TEM analyses were performed on the samples after solvent evaporation under vacuum, performed at room temperature for 2 h.

The surface morphology of the samples was investigated using a scanning electron microscope (SEM, LEO 1450VP), equipped with an X-ray probe (INCA Energy Oxford, Cu-Kα X-ray source, k = 1.540562 Å), in order to perform elemental analysis. The specimens (0.5 × 0.5 mm^2) were fractured in liquid nitrogen, fixed to conductive adhesive tapes and gold-metallized.

The thermo-oxidative stability of the samples was evaluated by thermogravimetric analyses (TGA) performed from 50 to 800 °C with a heating rate of 10 °C min^{-1}, using a Pyris1TGA Q 500 analyzer. The samples were placed in open alumina pans and analyzed in air atmosphere (flux: 60 mL min^{-1}).

Differential scanning calorimetry (DSC) scans were performed on a DSC Q20 TA Instrument, from −50 to 200 °C, with a heating rate of 20 °C min^{-1}. The samples were placed in closed 40 μL aluminium crucibles and analyzed in inert atmosphere (nitrogen flux: 40 mL min^{-1}).

Dynamic–mechanical thermal analyses (DMTA) were performed with a DMA Q800 TA Instrument. The measurements were carried out at a constant frequency of 1 Hz, strain amplitude of 15 μm with a preload of 0.01 N, and a temperature range from −90 to 180 °C, with a heating rate of 10 °C min^{-1}. Cylindrical samples (length: 35 mm, diameter: 4.8 mm) were analyzed in bending (dual cantilever) mode. Three DMTA tests were repeated for each material in order to have reproducible and significant data. Standard deviation for the storage modulus (E') values was within 5%.

Three point bending flexural tests, according to ASTM D790, were performed, using a Zwick-Roll Z010 apparatus, equipped with a 5 kN load cell, 30 mm support span, at 23 ± 2 °C and

This journal is © The Royal Society of Chemistry 2011

50 ± 5% relative humidity. At least five tests were repeated for each material in order to have reproducible and significant data.

Conclusions

In a recent review by Kim *et al.*,[27] the authors listed a number of challenges to be addressed in order to make graphene-based polymer nanocomposites really advantageous and exploitable in practical applications, namely: cost, handling of graphene sheets in processing, their purity and absence of defects, and adhesion between graphene and the polymer matrix. This work not only succeeded in all these issues, but also shows a method for producing graphene in the highest concentrations reached so far in any liquid; furthermore, this goal was achieved by directly using graphite and avoiding any chemical manipulation, which always results in defects still remaining on the graphene surface. In addition, for the first time a certain amount of graphene nanoribbons was also obtained by direct graphite sonication, a method that will be developed in our future work.

Specifically, a novel and simple method was successfully exploited for obtaining good "*in situ*" formed graphene/TEGDA dispersions and graphene/PTEGDA nanocomposites, thus limiting the reaggregation phenomena that may occur during the nanofiller recovery from a non-reactive solvent in traditional processes and lead to the undesired reaggregation to graphite flakes.

Raman spectroscopy demonstrated that the graphene directly formed within the acrylic monomer does not undergo oxidation to graphite oxide and is made of a very limited number of graphene layers. Regardless of their concentration in the polyacrylate network, a very homogeneous distribution of the graphene sheets within the PTEGDA matrix was obtained for all the systems investigated. DSC analyses and thermo-mechanical tests indicated the occurrence of strong polymer/filler interactions: in particular, a significant increase in the T_g values was assessed also in the presence of very low graphene content, together with a strong increase in flexural and storage moduli. Finally, the thermo-oxidative stability of the PTEGDA was not affected by the presence of graphene nanosheets.

Since the nanocomposite containing the highest graphene concentration (9.45 mg mL^{-1}) exhibits properties that approach those typical of the filler-free polymer, the corresponding highest concentration liquid dispersion might be used in copolymer synthesis in order to increase the final graphene content.

As a final remark, it should be highlighted that the real driving force for graphite exfoliation in liquid media is still not understood. Namely, TEGDA was used because it was found to be the most effective liquid in a series comprising (meth-)acrylic, silane, isocyanate, diol monomers and several other solvents. A thorough study on this aspect is in progress and will be reported soon.

References

1 P. R. Wallace, *Phys. Rev.*, 1947, **71**, 476.
2 K. S. Novoselov, A. K. Geim, S. V. Morozov, D. Jiang, Y. Zhang, S. V. Dubonos, I. V. Grigorieva and A. A. Firsov, *Science*, 2004, **306**, 666.
3 C. Lee, X. Wei, J. W. Kysar and J. Hone, *Science*, 2008, **321**, 385.
4 A. A. Balandin, S. Ghosh, W. Bao, I. Calizo, D. Teweldebrhan, F. Miao and C. N. Lau, *Nano Lett.*, 2008, **8**, 902.
5 K. I. Bolotin, K. J. Sikes, Z. Jiang, M. Klima, G. Fudenberg, J. Hone, P. Kim and H. L. Stormer, *Solid State Commun.*, 2008, **146**, 351.
6 M. D. Stoller, S. Park, Y. Zhu, J. An and R. S. Ruoff, *Nano Lett.*, 2008, **8**, 3498.
7 K. S. Novoselov, A. K. Geim, S. V. Morozov, D. Jiang, Y. Zhang, S. V. Dubonos, I. V. Grigorieva and A. Firsov, *Science*, 2004, **306**, 666.
8 C. Berger, Z. M. Song, X. B. Li, X. S. Wu, N. Brown, C. Naud, D. Mayou, T. Li, J. Hass, A. N. Marchenkov, E. H. Conrad, P. N. First and W. A. de Heer, *Science*, 2006, **312**, 1191.
9 X. Wang, L. Zhi, N. Tsao, Z. Tomovic, J. Li and K. Muellen, *Angew. Chem., Int. Ed.*, 2008, **47**, 2990.
10 S. Stankovich, D. A. Dirkin, R. D. Piner, K. A. Kohlhaas, A. Kleinhammes, Y. Jia, Y. Wu, S. T. Nguyen and R. S. Ruoff, *Carbon*, 2007, **45**, 1558.
11 Y. Hernandez, V. Nicolosi, M. Lotya, F. M. Blighe, Z. Y. Sun, S. De, I. T. McGovern, B. Holland, M. Byrne, Y. K. Gun'ko, J. J. Boland, P. Niraj, G. Duesberg, S. Krishnamurthy, R. Goodhue, J. Hutchison, V. Scardaci, A. C. Ferrari and J. N. Coleman, *Nat. Nanotechnol.*, 2008, **3**, 563.
12 N. Liu, F. Luo, H. Wu, Y. Liu and C. Zhang, *Adv. Funct. Mater.*, 2008, **18**, 1518.
13 N. Behabtu, J. R. Lomeda, M. J. Green, A. L. Higginbotham, A. Sinitskii, D. V. Kosynkin, D. Tsentalovich, A. N. G. Parra-Vasquez, J. Schmidt, E. Kesselman, Y. Cohen, Y. Talmon, J. M. Tour and M. Pasquali, *Nat. Nanotechnol.*, 2010, **5**, 406.
14 U. Khan, A. O'Neill, M. Lotya, S. De and J. N. Coleman, *Small*, 2010, **6**(7), 864.
15 M. Lotya, Y. Hernandez, P. J. King, R. J. Smith, V. Nicolosi, L. S. Karlsson, F. M. Blighe, S. De, Z. Wang, I. T. McGovern, G. S. Duesberg and J. N. Coleman, *J. Am. Chem. Soc.*, 2009, **131**, 3611.
16 P. Blake, P. D. Brimicombe, R. R. Nair, T. J. Booth, D. Jiang, F. Schedin, L. A. Ponomarenko, S. V. Morozov, H. F. Gleeson, E. W. Hill, A. K. Geim and K. S. Novoselov, *Nano Lett.*, 2008, **8**, 1704.
17 A. A. Green and M. C. Hersam, *Nano Lett.*, 2009, **9**, 4031.
18 D. Nuvoli, L. Valentini, V. Alzari, S. Scognamillo, S. Bittolo Bon, M. Piccinini, J. Illescas and A. Mariani, *J. Mater. Chem.*, 2011, **21**, 3428.
19 H. Podall, W. E. Foster and A. P. Giraitis, *J. Org. Chem.*, 1958, **30**, 82.
20 I. M. Panayotov and I. B. Rashkov, *J. Polym. Sci., Part A: Polym. Chem.*, 1973, **11**, 2615.
21 J. Parrod and G. Beinert, *J. Polym. Sci.*, 1961, **53**, 99.
22 L. R. Bunnell, Battelle Memorial Institute, 5186919, 1993.
23 Y. X. Pan, Z. Z. Yu, Y. C. Ou and G. H. Hu, *J. Polym. Sci., Part B: Polym. Phys.*, 2000, **38**, 1626.
24 P. Liu and K. Gong, *Carbon*, 1999, **37**, 701.
25 T. Kyotani, H. Moriyama and A. Tomita, *Carbon*, 1997, **35**, 1185.
26 M. Moniruzzaman and K. I. Winey, *Macromolecules*, 2006, **39**, 5194.
27 H. Kim, A. A. Abdala and C. W. Macosko, *Macromolecules*, 2010, **43**, 6515.
28 V. Alzari, D. Nuvoli, S. Scognamillo, M. Piccinini, E. Gioffredi, G. Malucelli, S. Marceddu, M. Sechi, V. Sanna and A. Mariani, *J. Mater. Chem.*, 2011, **21**(24), 8727.
29 A. C. Ferrari, *Solid State Commun.*, 2007, **143**, 47.
30 A. C. Ferrari, J. C. Meyer, V. Scardaci, C. Casiraghi, M. Lazzeri, F. Mauri, S. Piscanec, D. Jiang, K. S. Novoselov, S. Roth and A. K. Geim, *Phys. Rev. Lett.*, 2006, **97**, 187401.
31 X. Li, X. Wang, L. Zhang, S. Lee and H. Dai, *Science*, 2008, **319**, 1229.
32 Z. S. Wu, W. Ren, L. Gao, B. Liu, J. Zhao and H. M. Cheng, *Nano Res.*, 2010, **3**, 16.
33 L. Jiao, X. Wang, G. Diankov, H. Wang and H. Dai, *Nat. Nanotechnol.*, 2010, **5**, 321.
34 M. Terrones, A. R. Botello-Méndez, J. Campos-Delgado, F. López-Urías, Y. I. Vega-Cantú, F. J. Rodríguez-Macías, A. L. Elías, E. Munoz-Sandoval, A. G. Cano-Márquez, J. C. Charlier and H. Terrones, *Nano Today*, 2010, **5**, 351.
35 A. Mariani, D. Nuvoli, V. Alzari and M. Pini, *Macromolecules*, 2008, **41**, 5191.
36 M. Lotya, P. J. King, U. Khan, S. De and J. N. Coleman, *ACS Nano*, 2010, **4**, 3155.